TABLE I
TYPICAL CHANGES IN n INDUCED BY VACUUM OPERATION (n_0 IS IDEALITY FACTOR AT ATMOSPHERIC PRESSURE)

air pressure	$\frac{n}{n_0}$
open air	1
after 5 hrs. of .05 torr air immersion	0.66
after 1 week of .05 torr air immersion	0.55

Fig. 2 indicates barrier lowering due to the field is less in vacuum. This is also readily understood in terms of desorption. Adsorbed gas atoms are bonded rather weakly to the surface. Because of the weak bonds, impurities contributed by them to the semiconductor material are generally at *shallow* energy levels. These surface population states are thus much more susceptible to changes with bias. Fig. 2 is thus also consistent with the concept of desorption.

The increased barrier in vacuum would appear to be directly responsible for the tunneling decrease [9]. Similar experimental results were obtained with IN23B diodes.

As regards detection applications, it is also of interest to note that, as the current approaches pure thermionic emission, equivalent shot-noise temperature is known to decrease [9], thus increasing the signal-to-noise ratio (SNR) even further. Furthermore, the vacuum levels used in this study are quite modest. Desorption is known to vary linearly with pressure [10]–[13]. Consequently, further reductions in pressure should increase the barrier height still further. However, since barrier width also affects tunneling probability, it does not necessarily follow that lowest ambient pressure necessarily makes the diode more nearly ideal. No effort was made to determine vacuum pressure at which SNR is optimized.

This work indicates that conductivity, capacitance, and video detection and mixing sensitivity can be noticeably affected by surface effects such as *changing ambient pressure*. These should be considered in high altitude and space applications, as well as in packaging techniques.

REFERENCES

[1] N. S. Kopeika, H. Aharoni, I. Hirsh, S. Hava, and I. Lupo, "Wavelength tuning of GaAs LEDs through surface effects," *IEEE Trans. Electron. Device*, vol. ED-30, pp. 334–347, Apr. 1983.

[2] N. S. Kopeika, S. Hava, and I. Hirsh, "Gamma ray irradiated LED's: Surface emission and significant wavelength tuning through surface states," *IEEE J. Quantum Electron.*, vol. QE-20, pp. 63–71, Jan. 1984.

[3] N. S. Kopeika, I. Hirsh, and E. Hazout, "Significant photodiode quantum efficiency improvement and spectral response alteration through surface effects in vacuum," *IEEE Trans. Electron Devices*, vol. ED-31, pp. 1198–1205, Sept. 1984.

[4] Y. Makover, O. R. Manor, and N. S. Kopeika, "Very high sensitivity heterodyne detection of *X*-band radiation with neon indicator lamps," *IEEE Trans. Microwave Theory Tech.*, vol. MTT-26, pp. 38–41, Jan. 1978.

[5] Y. Kanda, "Effect of stress on germanium and silicon p-n junctions," *Japan J. Appl. Phys.*, vol. 6, pp. 475–486, Apr. 1967.

[6] J. R. Hauser and J. J. Wortman, "Some effects of mechanical stress on the breakdown voltage of p-n junctions," *J. Appl. Phys.*, vol. 37, pp. 3884–3892, Sept. 1966.

[7] E. H. Rhoderick, "Metal–semiconductor contacts," *Inst. Elec. Eng. Proc.*, vol. 129, pt. 1, pp. 1–14, Feb. 1982.

[8] V. L. Rideout, "A review of the theory, technology and applications of metal-semiconductor rectifiers," *Thin Solid Films*, vol. 48, pp. 261–291.

[9] M. V. Schneider, "Electrical characteristics of metal–semiconductor junctions," *IEEE Trans. Microwave Theory Tech.*, vol. MTT-28, pp. 1169–1173, Nov. 1980.

[10] P. A. Redhead, "Thermal desorption of gases," *Vacuum*, vol. 13, pp. 203–211, 1962.

[11] J. T. Law, "The adsorption of water vapor on germanium and germanium dioxide," *J. Phys. Chem.*, vol. 59, pp. 62–71, Jan. 1955.

[12] J. T. Law, "The adsorption of gases on a germanium surface," *J. Phys. Chem.*, vol. 59, pp. 543–548, June 1955.

[13] R. H. Kingston, "Water vapor induced n-type surface conductivity on p-type germanium," *Phys. Rev.*, vol. 98, pp. 1766–1775, June 1955.

Effect of Inner Conductor Offset in a Coplanar Waveguide

KOHJI KOSHIJI AND EIMEI SHU

***Abstract*—This paper reports on the effect of structural offset in a coplanar waveguide on the characteristic impedance and line loss. This effect can be an appreciable factor in designing highly precise circuits, such as MIC's using coplanar waveguide, or a coplanar-type standing-wave detector.**

The electric field over the cross section of the line is analyzed by assuming a TEM mode of wave propagation, and solving a two-dimensional Laplace's equation by means of the successive over-relaxation method. In the analysis, an approximate solution based on symmetry is employed. Also, measurements are made to confirm the results thus obtained.

I. INTRODUCTION

Coplanar waveguides are so composed as to make it especially convenient for constructing nonreciprocal circuit elements using magnetic substrates, as well as active circuit elements employing transistors and diodes.

Studies on the fundamental characteristics of coplanar waveguides have been made by C. P. Wen [1], T. Hatsuda [2], M. E. Davis *et al.* [3], J. B. Knorr *et al.* [4], Y. Fujiki *et al.* [5], and the authors [6]–[8]. This paper reports on the effect of structural offset in a coplanar waveguide on the line characteristics. This effect constitutes an appreciable factor in designing highly precise circuits, such as MIC's using coplanar waveguide or a coplanar-type standing-wave detector. In this report, changes in the characteristic impedance and line losses as a result of offset are evaluated by solving Laplace's equation. Computer solution of Laplace's equation is conducted by means of the successive over-relaxation method. Also, measurements are made to confirm the results obtained.

II. METHOD OF ANALYSIS

Fig. 1 shows the cross section of a coplanar waveguide, in which the width of the inner conductor is denoted by $2w$, the spacings between the inner and the outer conductors by s_1 and s_2, and the thickness of the conductors by $2t$. The conductors are supported by a dielectric substrate of thickness d, relative permittivity ϵ_r, and unit relative permeability.

The first step of the analysis is to determine the electric field over the cross section of the line. This problem can be reduced to that of a two-dimensional static field if we assume a TEM mode

Manuscript received August 12, 1983; revised April 13, 1984.

The authors are with the Faculty of Science and Technology, Science University of Tokyo, Noda-shi, 278, Japan.

0018-9480/84/1000-1387$01.00 ©1984 IEEE

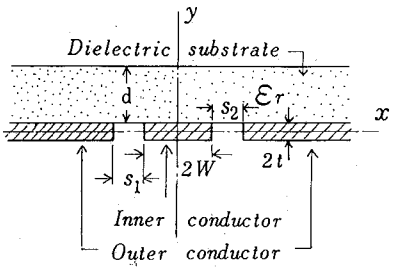

Fig. 1. Cross section of the coplanar waveguide.

of wave propagation. In other words, the potential distribution is a solution of Laplace's equation in two dimensions. To give the boundary values necessary for solving Laplace's equation, a shielding wall of zero potential is assumed. It is located sufficiently far away from the most critical part of the line, that is, near the gaps between the inner and outer conductors, so that it does not appreciably affect the field distribution of the essential line configuration shown in Fig. 1.

In order to give the measure of how much the inner conductor is deviated from its center position, let us define the offset index Δs of a coplanar waveguide as follows:

$$\Delta s = \frac{|s_1 - s_2|}{s_1 + s_2}. \tag{1}$$

With respect to the coplanar waveguide shown in Fig. 1, the line parameters have been evaluated for the case in which Δs is equal to zero ($s_1 = s_2$) [6]–[8]. In these papers, it is shown that, because of symmetry in the line construction, fairly accurate results can be obtained, with or without the substrate present, even if the region of computation is limited to only a quarter of the line cross-sectional area.

Now, consider a case in which the inner conductor deviates to the right or left, but with $s_1 + s_2 (= 2s)$ kept unchanged. In this case, the line construction is no longer symmetrical with respect to the y-axis. With respect to the x-axis, however, an approximate solution based on symmetry is possible as described in papers [6]–[8]. The approximation consists in synthesizing one solution with another. The first one is the half-region (above or below the x-axis) solution for the substrate-free case (Fig. 2(a)), and the second one is the solution in the same region obtained for a line construction in which the substrate extends symmetrically on both sides of the x-axis (Fig. 2(b)). It has been shown in papers [6], [8] that this approximation is sufficiently accurate for practical purposes.

In order to carry out computation by the successive overrelaxation method, the upper-half or lower-half region in Fig. 1 is divided into small sections with 257×129 mesh points. Unit potential and zero potential are assigned to the inner and outer conductors, respectively, as the boundary values. As for the boundaries along the x-axis between the inner and outer conductors, it is not necessary to assign specific potentials along them because they lie on the axis of symmetry and the potential can be evaluated from those at the adjacent points.

TABLE I
PARAMETERS USED IN CALCULATION

Number of mesh points	257 x 129	321 x 57 (subdivided)
Number of divisions in the "w+s" section	20	80

w/s	From	0.25	to	4.0
t/(w+s)	From	0	to	0.2
d/(w+s)	From	0	to	1.6
ε_r	1.0,	2.7		

Next, in regard to all these points, the relaxation process is repeated until the sum total of amounts of correction at all points as a result of a single relaxation process reduces to 10^{-5} or less. Then, part of the region thus analyzed (containing 81×15 mesh points), which includes the inner conductor, part of the outer conductor and the gap between them, is further divided into much smaller sections with 321×57 mesh points, so that the mesh spacing reduces to one fourth that of the original section. In this subdivided region, for which the boundary values can be obtained from the result of the previous computation, the relaxation process stated above is again repeated until the sum total of amounts of correction at all points as a result of a single relaxation process reduces to 10^{-5} or less. The last state thus attained is regarded as the true potential distribution. From the potential distribution determined in this way, it is possible to obtain line parameters, such as characteristic impedance and the dielectric and conductor losses [6]–[8]. In Table I, the dimensions of the line constructions analyzed and the permittivity of the substrates used are listed.

III. Results of Calculation and Measurement

Figs. 3, 4, and 5 show typical examples, respectively, of the characteristic impedance, conductor loss, and dielectric loss, all calculated for the case of zero offset [6]–[8]. In Fig. 4, α_c is the conductor loss per unit length in nepers per meter, Rs the surface resistance of the conductor, and ξ the length per section when the actual length of $w + s$ is divided into 20 equal sections. In Fig. 5, α_d is the dielectric loss per unit length in nepers per

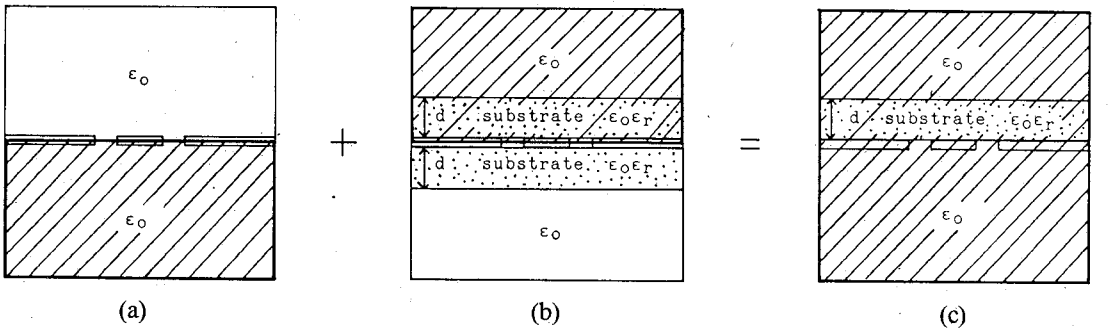

Fig. 2. (a) First solution, (b) second solution, and (c) synthesized solution.

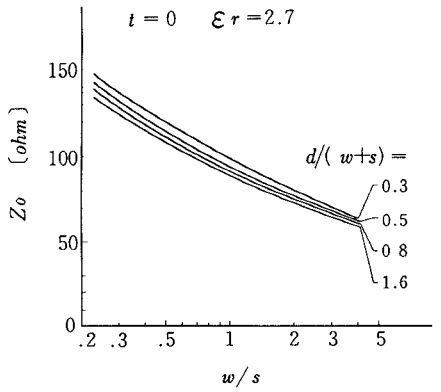

Fig. 3. Characteristic impedance for nonoffset line obtained from the analysis.

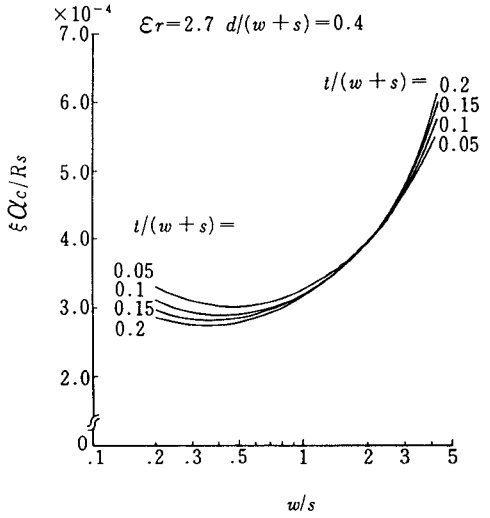

Fig. 4. Attenuation constant α_c due to conductor loss for nonoffset line.

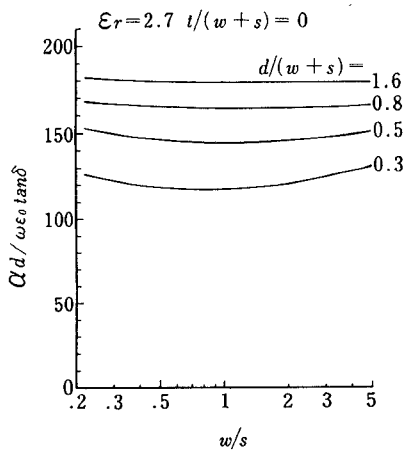

Fig. 5. Attenuation constant α_d due to dielectric loss for nonoffset line.

meter, ω the angular frequency, ϵ_0 the permittivity of free space, and $\tan\delta$ the dielectric loss tangent of the substrate used.

To estimate the line loss using graphs such as Figs. 4 and 5, first determine structural parameters t, w, s, and d, as well as material parameters Rs, ϵ_r, and $\tan\delta$ with a given value of angular frequency ω. Then, read the ordinate of the graph corresponding to w/s. The value of ordinate thus obtained is multiplied by Rs/ξ to give α_c (Fig. 4), or multiplied by $\omega\epsilon_0\tan\delta$ to give α_d (Fig. 5), ξ being equal to $(w+s)/20$.

TABLE II
COMPARISON WITH THE RESULTS OF PAPER [3]

d/(w+s)=0.5 εr=10.0 w/s=1.0 Δs=0

	Authors	M. E. Davis, et al.[3]
Relative phase velocity	0.49	0.48
Characteristic impedance	58.9	57.7

d/(w+s)=1.5 εr=10.0 w/s=1.0 Δs=0

	Authors	M. E. Davis, et al.[3]
Relative phase velocity	0.44	0.43
Characteristic impedance	52.3	52.4

Table II shows, for the nonoffset case, characteristic impedances obtained by means of the approximation computation stated in this paper, as compared with those based on paper [6].

Fig. 6(a), (b), and (c) shows characteristic impedance $\overline{Z_0}$, conductor loss $\overline{\alpha_c}$, and dielectric loss $\overline{\alpha_d}$, as a function of offset index Δs, respectively. Here $\overline{Z_0}$, $\overline{\alpha_c}$, and $\overline{\alpha_d}$ are all normalized by their corresponding values for the nonoffset case. In all these figures, characteristic impedance $\overline{Z_0}$ is seen to be decreasing with increasing value of Δs. This is because, as Δs increases, the gap on one side of the inner conductor gets narrower while the gap on the other side widens, and the increase in capacitance on one side more than compensates for the decrease on the other, thus making the overall capacitance tend to increase. On the other hand, conductor loss tends to increase with increasing value of Δs, because the line current is unequally divided between the two sides of the inner conductor. As for dielectric loss, variation with Δs is not so remarkable, as in the case of characteristic impedance or conductor loss. This is due to the fact that the ratio of the amount of electric fluxes passing through the substrate-filled region to those passing through the substrate-free region is almost fixed, irrespective of the amount of offset.

Figs. 7 and 8 show characteristic impedance and line loss, respectively, measured for a number of coplanar waveguides of different offset indices. As it is rather difficult to make coplanar IC's of practical size, all measurements were made for waveguides of enlarged dimensions and similar configurations. In all of the waveguides we made, $2w + s_1 + s_2$ has a fixed value of 6.0 mm.

As shown in Fig. 7, the measured value of characteristic impedance is found to be within 10 percent of the calculated value for $0 \leqslant \Delta s \leqslant 0.8$.

In Fig. 8, which shows results of measurement of the overall attenuation constant $\alpha_c + \alpha_d$, the relative error of the measured values as compared with the calculated value is found to be less than 11 percent. However, trend of variation of line loss with Δs is rather indistinct.

The above measurements were all carried out by the method described in the literature [6]–[8].

To interpret the results of our calculation in terms of the actual dimensions of an MIC, for example, consider a coplanar waveguide in which $s_1 = s_2 = 50$ μm, $w = 50$ μm, $t = 2$ μm, $\epsilon_r = 2.7$, and $d = 50$ μm. If we assume that the inner conductor is deviated to the right or left by 5 μm, or 0.1 in terms of offset index, then the characteristic impedance will be reduced by about 0.5 percent. In other words, in order to keep the error in characteristic

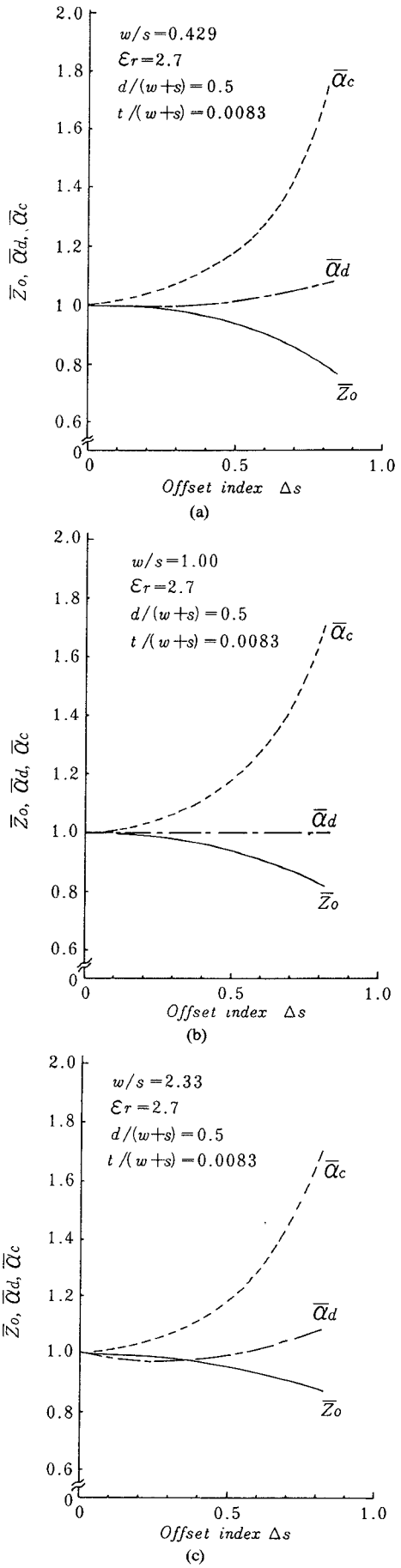

Fig. 6. Characteristic impedance and line losses as a function of offset index.

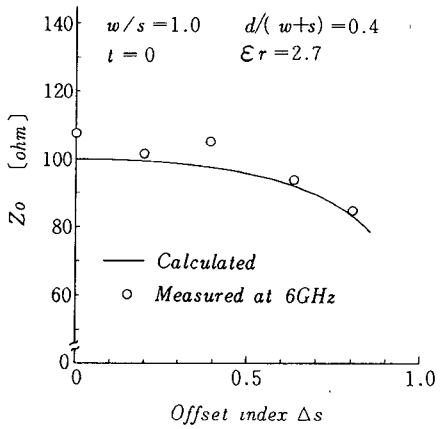

Fig. 7. Characteristic impedance obtained from measurement.

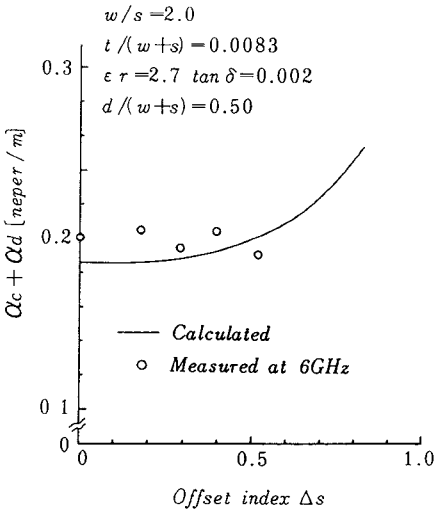

Fig. 8. Overall line loss obtained from measurement.

impedance within 0.5 percent, mechanical precision must be so high as to keep the amount of inner conductor offset less than about 5 μm.

REFERENCES

[1] C. P. Wen, "Coplanar waveguide: A surface strip transmission line suitable for nonreciprocal gyromagnetic device application," *IEEE Trans. Microwave Theory Tech.*, vol. MTT-17, pp. 1087–1090, Dec. 1969.

[2] T. Hatsuda, "Computation of coplanar-type strip lines characteristics by relaxation method," *Elec. Commun.* (Japan), vol. 54-B, pp. 661–668, Oct. 1971.

[3] M. E. Davis, E. W. Williams, and A. C. Celestini, "Finite-boundary corrections to the coplanar waveguide analysis," *IEEE Trans. Microwave Theory Tech.*, vol. MTT-21, pp. 594–596, Sept. 1973.

[4] J. B. Knorr and K. Kuchler, "An analysis of coupled slots and coplanar strips on dielectric substrate," *IEEE Trans. Microwave Theory Tech.*, vol. MTT-23, pp. 541–548, July 1975.

[5] Y. Fujiki, Y. Hayashi, M. Suzuki, and T. Kitazawa, "Higher order modes in coplanar-type transmission lines," *Elec. Commun.* (Japan), vol. J58-B, pp. 61–67, Feb. 1975.

[6] K. Koshiji, E. Shu, and S. Miki, "Analysis of coplanar waveguides with finite conductor thickness: Computation and measurement of characteristic impedances," *Elec. Commun.* (Japan), vol. J64-B, pp. 854–861, Aug. 1981.

[7] K. Koshiji, E. Shu, and S. Miki, "Dielectric and conductor losses in coplanar waveguides," *Elec. Commun.* (Japan), vol. J65-B, pp. 1499–1506, Dec. 1982.

[8] K. Koshiji, E. Shu and S. Miki, "Simplified computation of coplanar waveguide with finite conductor thickness," *IEE Proc.*, vol. 130, pt. H, pp. 315–321, Aug. 1983.